



Published in final edited form as:

J Neurochem. 2014 August ; 130(3): 351–359. doi:10.1111/jnc.12733.

Voltammetric and Mathematical Evidence for Dual Transport Mediation of Serotonin Clearance *In Vivo*

Kevin M. Wood^a, Anisa Zeqja^a, H. Frederik Nijhout^b, Michael C. Reed^c, Janet Best^d, and Parastoo Hashemi^{a,1}

^aDepartment of Chemistry, Wayne State University, 5101 Cass Avenue, Detroit, Michigan 48202, USA

^bDepartment of Biology, Duke University, Durham, NC, 27708, USA

^cDepartment of Mathematics, Duke University, Durham, NC, 27708, USA

^dDepartment of Mathematics, The Ohio State University, Columbus, 43201, OH, USA

Abstract

The neurotransmitter serotonin underlies many of the brain's functions. Understanding serotonin neurochemistry is important for improving treatments for neuropsychiatric disorders such as depression. Antidepressants commonly target serotonin clearance via serotonin transporters (SERTs) and have variable clinical effects. Adjunctive therapies, targeting other systems including serotonin autoreceptors, also vary clinically and carry adverse consequences. Fast scan cyclic voltammetry (FSCV) is particularly well suited for studying antidepressant effects on serotonin clearance and autoreceptors by providing real-time chemical information on serotonin kinetics *in vivo*. However, the complex nature of *in vivo* serotonin responses makes it difficult to interpret experimental data with established kinetic models. Here, we electrically stimulated the mouse medial forebrain bundle (MFB) to provoke and detect terminal serotonin in the substantia nigra reticulata (SNr). In response to MFB stimulation we found three dynamically distinct serotonin signals. To interpret these signals we developed a computational model that supports two independent serotonin reuptake mechanisms (high affinity, low efficiency reuptake mechanism and low affinity, high efficiency reuptake system) and bolsters an important inhibitory role for the serotonin autoreceptors. Our data and analysis, afforded by the powerful combination of voltammetric and theoretical methods, gives new understanding of the chemical heterogeneity of serotonin dynamics in the brain. This diverse serotonergic matrix likely contributes to clinical variability of antidepressants.

Keywords

Michaelis-Menten; 5-HT; Methiothepin; Computational Neuroscience; SERT; Transport

¹To whom correspondence should be addressed: phashemi@chem.wayne.edu.

Introduction

Serotonin is an important neurotransmitter because of its involvement in depression, which lowers mood and self-esteem and is among the most prevalent health problems in the USA (Gonzalez *et al.* 2010). The most popular antidepressants are the selective serotonin reuptake inhibitors (SSRIs). SSRIs inhibit serotonin transporters (SERTs), which extend the lifetime of serotonin in the synapse. These agents can take weeks to reach clinical effectiveness (Gelenberg & Chesen 2000), have variable benefits and carry harsh side effects (Cipriani *et al.* 2009, Ferguson 2001, Masand & Gupta 2002). Moreover, many patients fail to experience full remission after antidepressant therapy (Souery *et al.* 2006); thus, supplemental therapies targeting the serotonin autoreceptors, in addition to dopaminergic and noradrenergic receptors, are often co-prescribed with SSRIs (Davies *et al.* 2004, Richelson & Souder 2000, Alexander *et al.* 2011). The clinical effectiveness of these adjunctive strategies, such as the atypical antipsychotics Abilify™ and Seroquel™, remains variable (Spiekmans *et al.* 2013) and their mode of action is not well understood in depression (Yatham *et al.* 2005). It is likely that their impact on the serotonin autoreceptors is important because a wealth of literature implicates the autoreceptors in antidepressant mechanisms (Blier *et al.* 1987, Le Poul *et al.* 1995, Riad *et al.* 2004, Chaput *et al.* 1986). Therefore the neurochemistry that underlies serotonin release and transport is a critical field of study to better understand antidepressant mechanisms.

Fast scan cyclic voltammetry (FSCV) is a powerful tool for studying real-time neurochemistry in a living mammalian nervous system. FSCV has uncovered differences between serotonin and dopamine regulation *in vivo* (Hashemi *et al.* 2012). Briefly, serotonin is highly regulated, difficult to evoke electrically, and is mechanistically more driven by reuptake and metabolism than synthesis and vesicular packaging (Hashemi *et al.* 2012). Acute SSRI administration in mice rapidly decreases serotonin clearance. This process is not static but changes dynamically over 2 hours (Wood & Hashemi 2013). In contrast, acute serotonin autoreceptor antagonism had modest effects on serotonin release amplitude and clearance (Hashemi *et al.* 2012). From these studies, it is clear that the chemical cascades following SSRI and autoreceptor treatments are complicated. Understanding this chemistry is the key to designing better pharmacological agents. The first step towards this goal is to investigate endogenous serotonin clearance and autoreceptor control.

In this work we utilized FSCV to measure serotonin in the mouse substantia nigra pars reticulata (SNr) upon medial forebrain bundle (MFB) stimulation. We discovered a phenomenon that may better direct antidepressant studies. We found three distinct serotonin responses to the same electrical stimulation. We term these responses fast, slow, and hybrid based on differences in clearance curves.

By extending prior models that study serotonin kinetics in tissue slice preparations (Bunin *et al.* 1998, Bunin & Wightman 1998), we developed a Michaelis-Menten kinetic model to interpret our *in vivo* data. Our mathematical model showed that the three distinct responses can be understood as different combinations of two clearance or 'reuptake' mechanisms, one with high affinity and low efficiency and one with low affinity and high efficiency. Indeed, in 1970, Snyder and coworkers proposed two distinct reuptake mechanisms for serotonin,

which they termed “Uptake 1” and “Uptake 2” (Shaskan & Snyder 1970). More recently, Daws and coworkers pharmacologically distinguished between the transporters responsible for Uptake 1 and 2 and outlined the importance of targeting non-SERT transporters in antidepressant therapies (Daws *et al.* 2013, Horton *et al.* 2013). The kinetics of our two reuptake mechanisms agree well with Uptake 1 and 2. We found that administration of Escitalopram, a popular SSRI, not only largely inhibited Uptake 1 mechanisms but also, to a lesser extent, inhibited Uptake 2 mechanisms. Our model additionally showed that a strong autoreceptor effect is necessary to explain a descent of extracellular serotonin below baseline after stimulation. Autoreceptor modulation was confirmed experimentally by treating mice with methiothepin, an autoreceptor antagonist, which abolished serotonin’s descent below baseline. This finding is the first rapid chemically resolved evidence of autoreceptor function.

Our voltammetric experiments and computational analyses present three dynamic serotonin clearance patterns, support two distinct reuptake mechanisms for serotonin and suggest that serotonin is under a rapid, sophisticated level of autoreceptor control. Combined, our novel approach is a powerful platform from which to study the highly complex serotonergic release and reuptake machinery.

Methods and Materials

Animals

Male C57BL/6J mice (Jackson Laboratory, ME) weighing 20–25 g were used in stereotaxic surgeries (David Kopf Instruments, CA). Animal procedures were in agreement with *The Guide for the Care and Use of Laboratory Animals*, accepted by the Institutional Animal Care and Use Committees (IACUC) of Wayne State University. Mice were housed in 12 hr light/dark cycles and were presented food and water *ad libitum*.

Surgical Procedures

Before surgery, mice were injected into the intraperitoneal space with 25% urethane dissolved in 0.9% sodium chloride (Hospira, IL) at a volume of 7 μ L per 1 g mouse weight. Ideal mouse body temperature (37° C) was maintained using a heating pad (Braintree Scientific). Surgeries were performed on a stereotaxic frame (David Kopf Instruments, CA). A stainless steel stimulating electrode (diameter: 0.2 mm; Plastics One, VA) was implanted into the MFB and a microelectrode coated with Nafion (Hashemi *et al.* 2009) was lowered into the SNr as in previous studies (Wood & Hashemi 2013). Bregma was used as reference for stereotaxic coordinates of MFB [AP: -1.58, ML: 1.10, DV: -4.8 – 5.0] and SNr [AP: -3.28, ML: 1.40, DV: -4.2] from Franklin and Paxinos (Paxinos & Franklin 2008). Holes were drilled to access the SNr and MFB. Hydrochloric acid (0.1 M, 4 V vs tungsten) was used to electroplate chloride onto a silver wire (diameter: 0.010 in; A-M Systems, WA). The resulting Ag/AgCl reference electrode was positioned in the opposite hemisphere of the hole drilled for the SNr electrode placement. A 60 Hz biphasic 350 μ A, 120 pulse stimulation, 2 ms per phase was employed through a linear constant current stimulus isolator (NL800A Neurolog,; Digitimer Ltd, AL). Methiothepin mesylate (20 mg kg^{-1}) and Escitalopram

oxalate (100 mg kg^{-1}) were dissolved in saline and injected into the intraperitoneal cavity and obtained from Sigma Aldrich (St. Louis, MO).

Electrochemical Procedures

The carbon fiber microelectrodes were prepared by aspiration of carbon fibers (T- 650; diameter: $7 \mu\text{m}$; Goodfellow, PA) into glass capillaries (external diameter: 0.6 mm, internal diameter: 0.4 mm; A-M Systems). The filled glass capillaries were then pulled under gravity in a micropipette puller (Narishige Group, Tokyo). The carbon fibers distended from the glass capillaries were cut to approximately $150 \mu\text{m}$ and were subsequently coated with Nafion. Electrodeposition of Nafion was formerly described (Hashemi et al. 2009). Data acquisition and waveform application were performed via a PCIe-6341 DAC/ADC card (National Instruments, TX). Custom hardware and software (WCCV 2.0) written by Christopher W. Atcherley and Michael L. Heien using LabVIEW 2012 (National Instruments, TX) was used for voltammetry. A CHEM-CLAMP potentiostat (Dagan Corporation, MN) was used to measure current. For serotonin detection the carbon fiber microelectrode was scanned at 1000 V s^{-1} at 10 Hz from -0.1 V to 1.0 V , while holding at 0.2 V (Jackson *et al.* 1995). The calibration factor of serotonin for these electrodes and with the aforementioned waveform was taken from Hashemi *et al.* (Hashemi et al. 2009).

Flow Injection Analysis

A short 1/8 nut (PEEK P-335, IDEX, Middleboro, MA) was used to secure a nafion-electrocoated carbon-fiber microelectrode. The electrode/nut assembly was screwed onto a modified HPLC elbow joint (Elbow, PEEK 3432, IDEX, Middleboro, MA) connected to the output of the flow injection analysis (FIA) system. The FIA system is a six-port HPLC injector with a two-position actuator (Rheodyne model 7010 valve and 5701 actuator). Tris buffer (for constituents see (Hashemi *et al.* 2011b)) was used as the flow injection buffer at a flow rate of 2 mL min^{-1} via a syringe infusion pump (kd Scientific, model KDS-410, Holliston, MA). Serotonin hydrochloride was injected at fixed volume into the flow stream and reached the electrode as a square injection.

Data Modeling

The simulations were carried out in MatLab R2011a using ODE solver ode23s, implemented on an iMAC with operating system OS X Version 10.6.8.

Data Analysis

Custom software was written for data analysis in Labview. 2012 by Christopher Atcherley and Michael Heien (University of Arizona). The data was firstly background subtracted to remove a large capacitive current, a consequence of the high scan rates employed. The data was then filtered at zero phase using a fourth order Butterworth with a low pass of 5 kHz. $T_{1/2}$ analysis was performed on serotonin concentration ([serotonin]) vs. time traces using an automated peak finder function with eDAQ Chart software and peak parameters for $t_{1/2}$ analysis (eDAQ, Melbourne, Australia). Students t-tests were performed in excel on paired data sets, $p < 0.05$ was taken as statistically significant.

Results

Electrically Stimulated In Vivo Serotonin Responses

Three different serotonin responses were observed in the mouse SNr after biphasic electrical MFB stimulation (60 Hz, 120 pulses, 350 μ A), Figure 1. Representative color plots are shown in Figure 1A. Color plots are constructed by displaying substrate identifying cyclic voltammograms (CVs), collected at 10 Hz, with time. The y-axis is potential, the x-axis is time and the z-axis is a false color scale denoting current. Average [serotonin] vs. time plots, taken from the horizontal dashed lines, are shown in Figure 1B. The green rectangles under the color plots and the [serotonin] vs. time plots show the duration of electrical stimulation. We termed these three responses fast (blue solid curve), slow (orange solid curve), and hybrid (green solid curve) based on the shape and slopes of the decay from the peak to the baseline (serotonin clearance). Fast responses decay rapidly ($t_{1/2}$ of clearance < 6 seconds) with a single slope, slow responses decay sluggishly ($t_{1/2}$ > 6 seconds) with a single slope and hybrid responses display two slopes, decaying with fast profile for a few seconds, and then switching to slow decay. Average $t_{1/2}$ of the clearance curves of slow responses was 7.8 ± 3.2 s ($n=5 \pm$ standard error of the mean (SEM)), 1.6 ± 0.6 s ($n=5 \pm$ SEM) for fast responses and 5.9 ± 1.2 s ($n=5 \pm$ SEM) for hybrid responses. Fast responses had significantly lower $t_{1/2}$ than both slow ($p<0.0001$) and hybrid ($p=0.007$). No statistically significant differences were observed in $t_{1/2}$ between slow and hybrid responses ($p=0.197$). The amplitude of fast responses was 13.6 ± 0.7 nM, slow responses 22.9 ± 2.5 nM ($n=5 \pm$ SEM) and hybrid responses 29.6 ± 5.5 nM ($n=5 \pm$ SEM). Fast responses had significantly lower amplitude than both hybrid ($p=0.017$) and slow ($p=0.005$). No significant difference in amplitude was observed between hybrid and slow responses ($p=0.291$). In 67 mice, we found that approximately 20% of responses were fast, 30% were slow, and 50% were hybrid.

To establish that the nature of the three response types is physiological, we tested the kinetic reproducibility of our electrodes in a flow injection analysis system. In Figure 4 we injected serotonin (1 μ M) onto eight electrodes. The responses are displayed as an average with SEM. There are negligible differences in electrode kinetics because of the small magnitude of the error bars in the rising portion of the injection.

Modeling In Vivo Voltammetric Serotonin Responses

Our model, shown below, employs Michaelis-Menten kinetics similarly to a model introduced by Wightman and colleagues to describe serotonin kinetics in SNr tissue preparations (Bunin & Wightman 1998). However, our model additionally incorporates two reuptake mechanisms, a basal concentration of serotonin and autoreceptor effects. $[S(t)]$ denotes the concentration of serotonin in the SNr extracellular space. We assume that $[S(t)]$ satisfies the differential equation:

$$\frac{d[S(t)]}{dt} = R(t)(1 - A(t)) - \alpha \frac{V_{max1}[S(t)]}{K_{m1} + [S(t)]} - \beta \frac{V_{max2}[S(t)]}{K_{m2} + [S(t)]}$$

where $R(t)$ is the rate of release and $A(t)$ is the fraction of stimulated autoreceptors. $R(t)$ does not represent the MFB stimulation but rather neuronal firing in the DRN and subsequent release of serotonin in the SNr. In our control models (no drugs), firing rises and decays quickly (but not instantaneously) in response to the stimulation because of the non-instantaneous excitation/relaxation of the MFB-DRN-SNr circuitry. $V_{\max 1};K_{m1}$ and $V_{\max 2};K_{m2}$ are the V_{\max} and K_m values of the two Michaelis-Menten reuptake mechanisms. $V_{\max 1};K_{m1}$ correspond to slow responses, while $V_{\max 2};K_{m2}$ correspond to fast responses. The constants α and β are the weights of the two reuptake mechanisms. For fast responses $\alpha=0$ and $\beta=1$, for slow responses $\alpha=1$ and $\beta=0$. For hybrid responses: α is taken as 1 at all times. We incorporate β in the following way: when $[S(t)]$ is > 44 nM, β is 0.03 and then decays linearly to 0 as $[S(t)]$ decreases from 44 nM to 39 nM and $\beta = 0$ when $[S(t)]$ is < 39 nM. This means that the reuptake associated with β is low affinity and therefore loses effectiveness at low concentrations. Thus, hybrid responses have contributions from both reuptake mechanisms.

Figure 1B shows the model curves (burgundy dotted) superimposed onto the three experimental serotonin response types (blue, orange and green solid curves). We found that the following V_{\max} and K_m values fit well to the experimental data: $V_{\max 1};K_{m1} = 17.5$ nM s^{-1} and 5 nM and $V_{\max 2};K_{m2} = 780$ nM s^{-1} and 170 nM respectively. The three simulations carried the same V_{\max} and K_m values but differed in the choices of α , β , and the $R(t)$ and $A(t)$ functions shown for each response in Figure 1C. For fast response simulations $\alpha = 0$, so only the reuptake represented by $V_{\max 2};K_{m2}$ was present. $R(t)$ rose linearly for two seconds and then decayed linearly over 4 seconds. $A(t)$ rose linearly after 12 seconds. For slow response simulations $\beta = 0$, such that only the reuptake represented by $V_{\max 1};K_{m1}$ was present. $R(t)$ rose linearly for three seconds and then returned immediately to baseline. $A(t)$ rose linearly after 12 seconds with a different slope than the fast responses. For hybrid response simulations both reuptake mechanisms were present. $R(t)$ rose rapidly, fell rapidly, subsequently reaching plateau and returned to baseline. $A(t)$ rose linearly after 12 seconds, again with a different slope than slow and fast responses.

To model the effects of a hybrid response after SSRI administration, we administered Escitalopram (ESCIT). Figure 2 shows averaged control serotonin responses (black solid curve, $n=5 \pm$ SEM error bars in grey) and averaged responses 120 minutes after ESCIT administration (100 mg kg^{-1} , shown by teal solid curve, $n=5 \pm$ SEM error bars in light teal). Electrical stimulation duration is denoted by the green bar under the traces. The models are superimposed onto both curves in the burgundy dotted curves. The variation of $A(t)$ and $R(t)$ with time for both curves are inset. The best fit was obtained when Uptake 1 was inhibited by 95% and Uptake 2 by 40%.

Contribution from the Serotonin Autoreceptors

A common feature of our stimulated serotonin release profiles is that [serotonin] ‘dips’ below baseline. In Figure 3A, a representative serotonin release event is shown. CV_a (inset, taken during the stimulation at point a) represents a typical serotonin CV (with some additional features due to co-release of histamine obtained in the SNr via MFB stimulation (Hashemi *et al.* 2011a). CV_b (taken at the point where [serotonin] dips below baseline, b)

resembles the concentration inverse of CV_a . When CV_b is reversed and superimposed onto CV_a , there is a good agreement confirming a reduction in [serotonin]. For our model, it was necessary to incorporate an increasing autoreceptor effect (starting 7 seconds after the beginning of stimulation the function $A(t)$ increases linearly) to account for the dip. Both cell body (5-HT1A) and terminal (5-HT1B) autoreceptors that are part of the dorsal raphe nucleus (DRN)-MFB-SNr circuit contribute to $A(t)$.

To test our model's suggestion of autoreceptor control experimentally, we treated mice with methiothepin, a non-selective serotonin receptor antagonist, with highest affinity for the serotonin autoreceptors (Monachon *et al.* 1972). Figure 3B (**left**), shows control (black curve) and the average effects of acute methiothepin (20 mg kg^{-1}) administration ($n=5 \pm \text{SEM}$) (purple curve). The maximum amplitude was unaffected by this drug: at $24.1 \pm 6.7 \text{ nM}$ pre-methiothepin and $26.3 \pm 5.0 \text{ nM}$ 60 min post methiothepin ($p=0.489$, $n=5 \pm \text{SEM}$). The $t_{1/2}$ increased from $3.2 \pm 1.1 \text{ s}$ to $19.9 \pm 5.9 \text{ s}$ at 60 min ($p=0.032$, $n=5 \pm \text{SEM}$). The control response was treated with the hybrid response model (burgundy dotted curve). We modeled the methiothepin treatment by setting the autoreceptor effect function, $A(t)$, to zero and choosing the release function, $R(t)$, shown in Figure 3B (**right**). It is clear, both experimentally and via our model, that methiothepin abolishes serotonin's descent below baseline.

Discussion

Three Serotonin Response Types In Vivo

Serotonin reuptake is a major focus of antidepressant agents. We previously reported stimulated [serotonin] vs. time in the SNr (Wood & Hashemi 2013) as a composite average of 5 experiments. Upon accumulation of more data sets, however, it became apparent that responses are heterogeneous, and averaging removes nuances that provide important information about serotonin neurochemistry. We found three distinct serotonin responses to a standard stimulation, primarily differentiated by the clearance slopes. Michael and colleagues found dopamine heterogeneity in the rising portion of extracellular concentration curves and proposed the terminology, slow, fast, and hybrid (Moquin & Michael 2011, Moquin & Michael 2009), which we adopted here. For serotonin, all three responses have a rapid rise. Fast responses are characterized by a rapid return to baseline, and slow responses are characterized by a more gradual return to baseline. Hybrid responses have both fast and slow attributes because they descend rapidly for a short time and then switch to slow decay.

Differences between electrode kinetics could account for erroneous assignment of our responses. We explore this in Figure 4. Here, serotonin ($1 \mu\text{M}$) was injected *in vitro* onto eight electrodes; the responses are shown averaged with SEM. While there are differences in the response amplitude between electrodes, the difference in electrode kinetics is negligible (evidenced by the small error in the initial rising portion of the response shown between the two vertical green dashed lines). Therefore it is likely that *in vivo* processes underlie our three response types.

Two Serotonin Reuptake Mechanisms

Visual inspection of our three serotonin response types shows two separate clearance slopes, suggesting involvement of two discrete reuptake mechanisms. Simple $t_{1/2}$ analysis did not allow us to distinguish between hybrid and slow responses, therefore we sought to employ kinetic models to determine any differences. However, we could not model our responses with models established for serotonin release in tissue slice preparations (Bunin et al. 1998). We found that incorporation of two separate reuptake mechanisms into our model, $V_{\max 1};K_{m1}$ and $V_{\max 2};K_{m2}$ allowed us to closely model our experimental data. Local stimulations in tissue slice preparations create a massive efflux of serotonin (Bunin & Wightman 1998, Bunin et al. 1998). In previous tissue slice experiments, serotonin clearance was apparently dominated by a reuptake mechanism that kinetically mirrors our values for $V_{\max 2};K_{m2}$ while contributions from $V_{\max 1};K_{m1}$ were reasonable to neglect. It is interesting that close inspection of [serotonin] vs. time traces in these previous experiments (Bunin et al. 1998) shows that at low concentrations (low nM) the experimental data deviate from established models. At these low concentrations serotonin begins to decay slowly, in a similar way to our slow responses, described more aptly by $V_{\max 1};K_{m1}$.

In the early 70's Snyder and colleagues suggested that serotonin clearance occurred via 2 reuptake mechanisms (Shaskan & Snyder 1970). They proposed Uptake 1 with high affinity and low efficiency and Uptake 2 with low affinity and high efficiency. Daws and colleagues verified pharmacologically that Uptake 1 is likely to occur primarily via the serotonin transporters (SERTs) on serotonergic neurons and that Uptake 2 includes other transporters on other cells including the dopamine transporter (DAT), the norepinephrine transporter (NET) and the organic cation transporter (OCT) (Horton et al. 2013, Daws et al. 2013). Here, for the first time, we present endogenous *in vivo* data to support the concept of Uptake 1 and 2. Indeed our values for $V_{\max 1};K_{m1}$ (17.5 nM s⁻¹ and 5 nM) and $V_{\max 2};K_{m2}$ (780 nM s⁻¹ and 170 nM) agree remarkably well with high affinity, low efficiency uptake (Uptake 1) and with low affinity, high efficiency uptake (Uptake 2) respectively.

In vivo serotonin release is known to be highly regulated, and [serotonin]_{evoked} is in the low nM range (Wood & Hashemi 2013, Hashemi et al. 2011a, Hashemi et al. 2009, Hashemi et al. 2012). Furthermore, it has been demonstrated that inhibiting serotonin reuptake and metabolism (with an SSRI and MAOI) leads to the potentially fatal serotonin syndrome (Hashemi et al. 2012). Therefore it is not remarkable for multiple reuptake mechanisms to be charged with clearing serotonin from the synapse. It is probable that physiologically released serotonin is at low enough concentrations such that low efficiency, high affinity SERTs on serotonergic neurons, Uptake 1, can reuptake serotonin effectively. However, if serotonin release exceeds a certain limit, it may diffuse to other transport mechanisms, which are not as selective for serotonin and therefore have low affinity, but operate at high efficiency (Uptake 2).

To probe the effects of a commonly prescribed SSRI mechanistically, we administered ESCIT at a high dose. We chose to administer 100 mgkg⁻¹ and compare data taken at 120 minutes after drug administration based on previous dose response experiments that showed maximal and lingering effects with this dose and at this time (Wood & Hashemi 2013).

Figure 2 shows the experimental data and corresponding models. SSRI administration substantially increased serotonin release and decreased its clearance, as previously seen (Wood & Hashemi 2013). This is not surprising since ESCIT is highly selective for the SERTs (Uptake 1). However, after considerable experimentation we found that our data was best fit with a model that included 95% inhibition of Uptake 1 and 40% inhibition of uptake 2. This is not surprising given that there is evidence that SSRIs have affinity for uptake 2 transporters. For example, ESCIT has been found to block NETs and have a significant effect upon OCT-sensitive serotonin uptake (Nguyen *et al.* 2013). Furthermore, many SSRIs inhibit the human plasma membrane monoamine transporter (PMAT), also an uptake 2 transporter (Haenisch & Bonisch 2010). Finally, Horton *et al.* found that, in the presence of fluvoxamine, blockage of Uptake 2 by Decynium-22 greatly raised both the extra-cellular 5-HT level and the clearance time (Horton *et al.* 2013).

It is important to note that the high dose of ESCIT in our experiment (100 mgkg^{-1}) exceeds the minimal effective dose required for behavioral effects in mice (12 mgkg^{-1}) (Sanchez *et al.* 2003). Although not likely to be encountered clinically, the high dose enables us to illustrate a central point in this work: that physiological deviations above normal extracellular serotonin concentration are cleared via SERTs, but larger deviations are cleared through combination of the SERTs and Uptake 2 transporters. Since different SSRIs have different chemical compositions, it is reasonable to expect that, at a given concentration, each blocks some percentage of Uptake 1 and a (presumably lower) percentage of Uptake 2. Thus one would expect that both peak response and clearance time would vary among different SSRIs.

Serotonin Autoreceptor Regulation of Serotonin Transmission

FSCV does not determine the baseline or steady state value of the extracellular serotonin concentration; this is an essential, previously unaccounted for, component of kinetic models for serotonin. The experimental curve for fast response (Figure 1) descends 10–20 nM below baseline. While we cannot know what the absolute levels are, our data imply that the steady state concentration of serotonin is between 10–20 nM; we therefore assumed $[\text{serotonin}]_{\text{baseline}}$ in our simulations as 20 nM. After completing simulations, we subtracted 20nM from the model curves so that we could compare them directly to the experimental curves that are plotted with baseline as 0 nM. The value of 20 nM is not surprising because previous estimations of basal neurotransmitter concentrations (Justice 1993) are now thought to have underestimated the true concentrations (Wang *et al.* 2010, Owesson-White *et al.* 2012). In Figure 1, and in most of our experimental data, [serotonin] dips below this baseline after stimulation has ceased. While a dip below baseline has previously been attributed to pH shifts for dopamine experiments (Venton *et al.* 2003), comparison of cyclic voltammograms suggests that this dip is, indeed, a substantial reduction in extracellular serotonin.

It was, again, not possible to utilize traditional models to account for this dip, likely due to the inherent differences between serotonin regulation in tissue slice preparations and *in vivo*. Autoreceptors are known to inhibit serotonin release (Barnes & Sharp 1999), in particular, prior FSCV studies in tissue slice preparations and chronoamperometry studies in

synaptosomes and *in vivo* have uncovered important, discrete roles for different autoreceptor subtypes (Daws *et al.* 2000, Daws *et al.* 1999, Threlfell *et al.* 2010, Hagan *et al.* 2012, Hopwood & Stamford 2001, Roberts & Price 2001). In tissue slice experiments autoreceptors likely function differently than in *in vivo* because the cell body-terminal connections are severed. *In vivo*, in our circuitry, serotonin released from the DRN cell bodies stimulates 5HT1A autoreceptors and serotonin released in SNr acts on 5HT1B autoreceptors (Barnes & Sharp 1999). Therefore, we postulated that our dip below baseline could be autoreceptor mediated. Indeed, the gradually increasing autoreceptor effect in the model captures the experimental data very well. This is novel chemical data that implies ambient autoreceptor effects and the time-scale on which they operate.

To experimentally test this autoreceptor hypothesis we employed methiothepin, a non-selective serotonin receptor antagonist with most affinity for the serotonin autoreceptors, to target the multiple autoreceptors that are involved in the DRN-SNr circuitry (Barnes & Sharp 1999). A prior FSCV study in DRN slices showed that combined 5HT1A and 5HT1B receptor antagonism produced greater serotonin efflux than targeting either receptor alone (Roberts & Price 2001). In our study, methiothepin greatly increased the $t_{1/2}$ of clearance of our experimental data and our model could fit the experimental data by removing $A(t)$. This simple, yet effective modeling strategy gives further evidence that autoreceptors may be acting within the timeframe of our collection window (30 seconds) to reduce serotonin transmission.

The advantage of our model is its simplicity; however, it carries limitations. The product term, $R(t)(1-A(t))$, cannot distinguish between lowering $R(t)$ and raising $A(t)$. For example, the autoreceptor effect may proceed earlier than 7 seconds after initiation of the stimulation. Here, we considered $R(t)$ as release in the absence of autoreceptors and $(1 - A(t))$ as the modification of release when the autoreceptors are stimulated. We assumed that $R(t)$ rapidly increased and decreased in correspondence to the stimulus and $A(t)$ increased gradually thereafter (Figure 1C). An additional limitation is that we cannot yet distinguish between the different serotonin autoreceptors. Finally, our data imply that basal serotonin levels are around 20 nM; this level needs to be verified independently with a method capable of reporting basal serotonin levels at carbon fiber microelectrodes. Addressing these three limitations requires method development, elaborate pharmacological experiments, a more sophisticated modeling approach (Reed *et al.* 2012) and is the focus of our future work.

We studied endogenous serotonin release and reuptake with FSCV. We took a novel mathematical approach by treating the data with Michaelis-Menten kinetics that incorporated two reuptake mechanisms, a baseline serotonin concentration, and autoreceptor functions. Experimentally, we discovered three serotonin chemical signatures which we termed fast, slow, and hybrid and mathematically we found that they could be explained with two reuptake mechanisms. We found a high affinity, low efficiency reuptake mechanism (Uptake 1), proposed to be via the SERTs and a low affinity, high efficiency reuptake system (Uptake 2) thought to represent the contribution of DATs, NETs, and OCTs. Additionally, we outlined a timeframe for the inhibitory role of autoreceptors. Combining voltammetric and theoretical approaches gives us an ideal tool to study serotonin's dual-uptake mechanisms and autoreceptor control. This capability will be

invaluable for characterizing the mechanisms of the pharmacological effects of existing antidepressant agents and to aid in the design of novel agents.

Acknowledgments

WSU start-up funds (PH), NSF grants EF-1038593 (HFN, MR), NSF agreement 0112050 through the Mathematical Biosciences Institute (JB, MR), an NSF CAREER Award (JB), the Alfred P. Sloan Foundation (JB) and NIH grant R01 ES019876 (DT) supported this research.

References

- Alexander GC, Gallagher SA, Mascola A, Moloney RM, Stafford RS. Increasing off-label use of antipsychotic medications in the United States, 1995–2008. *Pharmacoepidemiology and drug safety*. 2011; 20:177–184. [PubMed: 21254289]
- Barnes NM, Sharp T. A review of central 5-HT receptors and their function. *Neuropharmacology*. 1999; 38:1083–1152. [PubMed: 10462127]
- Blier P, de Montigny C, Chaput Y. Modifications of the serotonin system by antidepressant treatments: implications for the therapeutic response in major depression. *J Clin Psychopharmacol*. 1987; 7:24S–35S. [PubMed: 3323264]
- Bunin MA, Prioleau C, Mailman RB, Wightman RM. Release and uptake rates of 5-hydroxytryptamine in the dorsal raphe and substantia nigra reticulata of the rat brain. *J Neurochem*. 1998; 70:1077–1087. [PubMed: 9489728]
- Bunin MA, Wightman RM. Quantitative evaluation of 5-hydroxytryptamine (serotonin) neuronal release and uptake: an investigation of extrasynaptic transmission. *The Journal of neuroscience : the official journal of the Society for Neuroscience*. 1998; 18:4854–4860. [PubMed: 9634551]
- Chaput Y, de Montigny C, Blier P. Effects of a selective 5-HT reuptake blocker, citalopram, on the sensitivity of 5-HT autoreceptors: electrophysiological studies in the rat brain. *Naunyn-Schmiedeberg's archives of pharmacology*. 1986; 333:342–348.
- Cipriani A, Furukawa TA, Salanti G, et al. Comparative efficacy and acceptability of 12 new-generation antidepressants: a multiple-treatments meta-analysis. *Lancet*. 2009; 373:746–758. [PubMed: 19185342]
- Davies MA, Sheffler DJ, Roth BL. Aripiprazole: a novel atypical antipsychotic drug with a uniquely robust pharmacology. *CNS drug reviews*. 2004; 10:317–336. [PubMed: 15592581]
- Daws LC, Gerhardt GA, Frazer A. 5-HT_{1B} antagonists modulate clearance of extracellular serotonin in rat hippocampus. *Neurosci Lett*. 1999; 266:165–168. [PubMed: 10465699]
- Daws LC, Gould GG, Teicher SD, Gerhardt GA, Frazer A. 5-HT_{1B} receptor-mediated regulation of serotonin clearance in rat hippocampus in vivo. *J Neurochem*. 2000; 75:2113–2122. [PubMed: 11032901]
- Daws LC, Koek W, Mitchell NC. Revisiting serotonin reuptake inhibitors and the therapeutic potential of “uptake-2” in psychiatric disorders. *ACS chemical neuroscience*. 2013; 4:16–21. [PubMed: 23336039]
- Ferguson JM. SSRI Antidepressant Medications: Adverse Effects and Tolerability. *Prim Care Companion J Clin Psychiatry*. 2001; 3:22–27. [PubMed: 15014625]
- Gelenberg AJ, Chesen CL. How fast are antidepressants? *The Journal of clinical psychiatry*. 2000; 61:712–721. [PubMed: 11078031]
- Gonzalez, O.; Berry, JT.; Mcknight-Eily, LR.; Strine, T.; Edwards, KW.; Croft, JB. Morbidity and Mortality Weekly Report. Center for Disease Control and Prevention; Hyattsville, MD: 2010. Current Depression Among Adults - United States, 2006 and 2008.
- Haenisch B, Bonisch H. Interaction of the human plasma membrane monoamine transporter (hPMAT) with antidepressants and antipsychotics. *Naunyn Schmiedeberg's Arch Pharmacol*. 2010; 381:33–39. [PubMed: 20012264]
- Hagan CE, McDevitt RA, Liu Y, Furay AR, Neumaier JF. 5-HT_{1B} autoreceptor regulation of serotonin transporter activity in synaptosomes. *Synapse*. 2012; 66:1024–1034. [PubMed: 22961814]

- Hashemi P, Dankoski EC, Lama R, Wood KM, Takmakov P, Wightman RM. Brain dopamine and serotonin differ in regulation and its consequences. *Proc Natl Acad Sci U S A*. 2012; 109:11510–11515. [PubMed: 22778401]
- Hashemi P, Dankoski EC, Petrovic J, Keithley RB, Wightman RM. Voltammetric Detection of 5-Hydroxytryptamine Release in the Rat Brain. *Analytical Chemistry*. 2009; 81:9462–9471. [PubMed: 19827792]
- Hashemi P, Dankoski EC, Wood KM, Ambrose RE, Wightman RM. In vivo electrochemical evidence for simultaneous 5-HT and histamine release in the rat substantia nigra pars reticulata following medial forebrain bundle stimulation. *J Neurochem*. 2011a; 118:749–759. [PubMed: 21682723]
- Hashemi P, Walsh PL, Guillot TS, Gras-Najjar J, Takmakov P, Crews FT, Wightman RM. Chronically Implanted, Nafion-Coated Ag/AgCl Reference Electrodes for Neurochemical Applications. *ACS Chem Neurosci*. 2011b; 2:658–666. [PubMed: 22125666]
- Hopwood SE, Stamford JA. Multiple 5-HT(1) autoreceptor subtypes govern serotonin release in dorsal and median raphe nuclei. *Neuropharmacology*. 2001; 40:508–519. [PubMed: 11249960]
- Horton RE, Apple DM, Owens WA, et al. Decynium-22 enhances SSRI-induced antidepressant-like effects in mice: uncovering novel targets to treat depression. *The Journal of neuroscience : the official journal of the Society for Neuroscience*. 2013; 33:10534–10543. [PubMed: 23785165]
- Jackson BP, Dietz SM, Wightman RM. Fast-scan cyclic voltammetry of 5-hydroxytryptamine. *Anal Chem*. 1995; 67:1115–1120. [PubMed: 7717525]
- Justice JB Jr. Quantitative microdialysis of neurotransmitters. *J Neurosci Methods*. 1993; 48:263–276. [PubMed: 8105154]
- Le Poul E, Laaris N, Doucet E, Laporte AM, Hamon M, Lanfumey L. Early desensitization of somatodendritic 5-HT_{1A} autoreceptors in rats treated with fluoxetine or paroxetine. *Naunyn-Schmiedeberg's archives of pharmacology*. 1995; 352:141–148.
- Masand PS, Gupta S. Long-term side effects of newer-generation antidepressants: SSRIS, venlafaxine, nefazodone, bupropion, and mirtazapine. *Annals of clinical psychiatry : official journal of the American Academy of Clinical Psychiatrists*. 2002; 14:175–182. [PubMed: 12585567]
- Monachon MA, Burkard WP, Jalfre M, Haefely W. Blockade of central 5-hydroxytryptamine receptors by methiothepin. *Naunyn Schmiedeberg's Arch Pharmacol*. 1972; 274:192–197. [PubMed: 4340797]
- Moquin KF, Michael AC. Tonic autoinhibition contributes to the heterogeneity of evoked dopamine release in the rat striatum. *Journal of neurochemistry*. 2009; 110:1491–1501. [PubMed: 19627437]
- Moquin KF, Michael AC. An inverse correlation between the apparent rate of dopamine clearance and tonic autoinhibition in subdomains of the rat striatum: a possible role of transporter-mediated dopamine efflux. *J Neurochem*. 2011; 117:133–142. [PubMed: 21244425]
- Nguyen HT, Guiard BP, Bacq A, David DJ, David I, Quesseveur G, Gautron S, Sanchez C, Gardier AM. Blockade of the high-affinity noradrenaline transporter (NET) by the selective 5-HT reuptake inhibitor escitalopram: an in vivo microdialysis study in mice. *Br J Pharmacol*. 2013; 168:103–116. [PubMed: 22233336]
- Owesson-White CA, Roitman MF, Sombers LA, Belle AM, Keithley RB, Peele JL, Carelli RM, Wightman RM. Sources contributing to the average extracellular concentration of dopamine in the nucleus accumbens. *J Neurochem*. 2012; 121:252–262. [PubMed: 22296263]
- Paxinos, G.; Franklin, KB. *The Mouse Brain in Stereotaxic Coordinates*. Academic Press; Waltham, MA: 2008.
- Reed MC, Nijhout HF, Best JA. Mathematical insights into the effects of levodopa. *Front Integr Neurosci*. 2012; 6:21. [PubMed: 22783173]
- Riad M, Zimmer L, Rbah L, Watkins KC, Hamon M, Descarries L. Acute treatment with the antidepressant fluoxetine internalizes 5-HT_{1A} autoreceptors and reduces the in vivo binding of the PET radioligand [18F]MPPF in the nucleus raphe dorsalis of rat. *J Neurosci*. 2004; 24:5420–5426. [PubMed: 15190115]
- Richelson E, Souder T. Binding of antipsychotic drugs to human brain receptors focus on newer generation compounds. *Life sciences*. 2000; 68:29–39. [PubMed: 11132243]
- Roberts C, Price GW. Interaction of serotonin autoreceptor antagonists in the rat dorsal raphe nucleus: an in vitro fast cyclic voltammetry study. *Neurosci Lett*. 2001; 300:45–48. [PubMed: 11172936]

- Sanchez C, Bergqvist PB, Brennum LT, Gupta S, Hogg S, Larsen A, Wiborg O. Escitalopram, the S-(+)-enantiomer of citalopram, is a selective serotonin reuptake inhibitor with potent effects in animal models predictive of antidepressant and anxiolytic activities. *Psychopharmacology (Berl)*. 2003; 167:353–362. [PubMed: 12719960]
- Shaskan EG, Snyder SH. Kinetics of serotonin accumulation into slices from rat brain: relationship to catecholamine uptake. *The Journal of pharmacology and experimental therapeutics*. 1970; 175:404–418. [PubMed: 5481708]
- Souery D, Papakostas GI, Trivedi MH. Treatment-resistant depression. *The Journal of clinical psychiatry*. 2006; 67(Suppl 6):16–22. [PubMed: 16848672]
- Spielmanns GI, Berman MI, Linardatos E, Rosenlicht NZ, Perry A, Tsai AC. Adjunctive atypical antipsychotic treatment for major depressive disorder: a meta-analysis of depression, quality of life, and safety outcomes. *PLoS medicine*. 2013; 10:e1001403. [PubMed: 23554581]
- Threlfell S, Greenfield SA, Cragg SJ. 5-HT(1B) receptor regulation of serotonin (5-HT) release by endogenous 5-HT in the substantia nigra. *Neuroscience*. 2010; 165:212–220. [PubMed: 19819310]
- Venton BJ, Michael DJ, Wightman RM. Correlation of local changes in extracellular oxygen and pH that accompany dopaminergic terminal activity in the rat caudate-putamen. *J Neurochem*. 2003; 84:373–381. [PubMed: 12558999]
- Wang Y, Moquin KF, Michael AC. Evidence for coupling between steady-state and dynamic extracellular dopamine concentrations in the rat striatum. *Journal of neurochemistry*. 2010; 114:150–159. [PubMed: 20403079]
- Wood KM, Hashemi P. Fast-Scan Cyclic Voltammetry Analysis of Dynamic Serotonin Responses to Acute Escitalopram. *ACS Chem Neurosci*. 2013
- Yatham LN, Goldstein JM, Vieta E, Bowden CL, Grunze H, Post RM, Suppes T, Calabrese JR. Atypical antipsychotics in bipolar depression: potential mechanisms of action. *The Journal of clinical psychiatry*. 2005; 66(Suppl 5):40–48. [PubMed: 16038601]

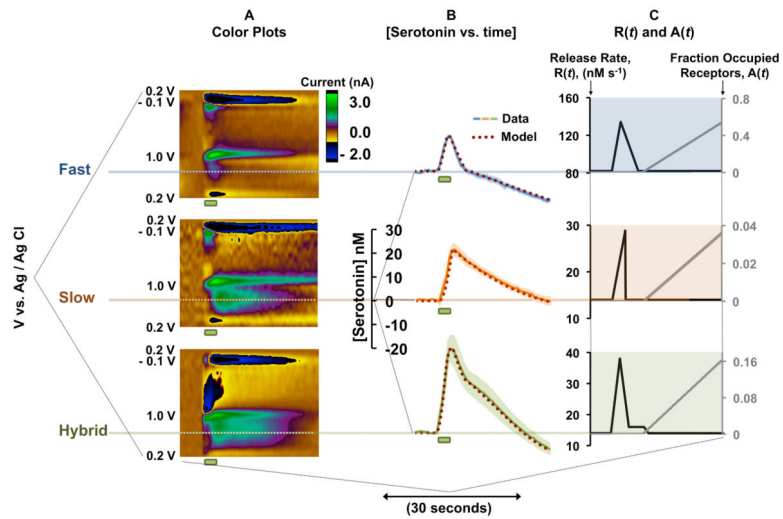


Figure 1.

A – Representative color plots for fast, slow and hybrid responses. Stimulation is denoted by green bar under each color plot. **B** – Averaged [serotonin] vs. time (solid curves, $n = 5 \pm$ SEM) and modeled curve (burgundy dotted) for the three response types. Stimulation is denoted by green bar under each plot. **C** – Choices of $R(t)$ and $A(t)$ for fast, slow and hybrid responses.

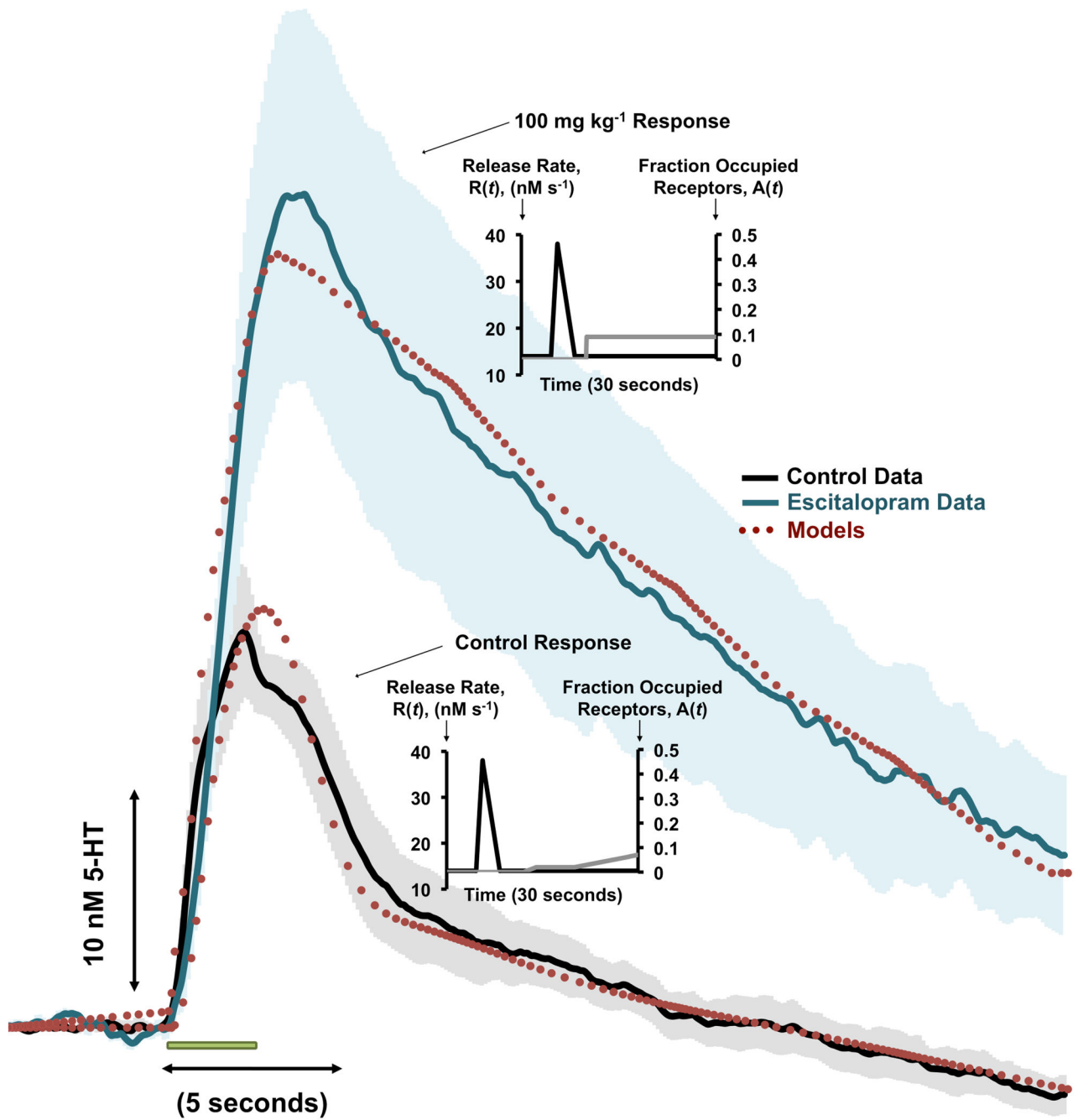


Figure 2.

A – Averaged [serotonin] vs. time trace for a control serotonin response (black curve, $n=5 \pm$ SEM) and 120 minutes after 100 mg kg⁻¹ ESCIT administration (teal curve, $n=5 \pm$ SEM). Stimulation duration is denoted by the green bar under the traces. The models are superimposed onto the traces in the burgundy dashed traces. Choices of $A(t)$ and $R(t)$ are inset for control and ESCIT responses.

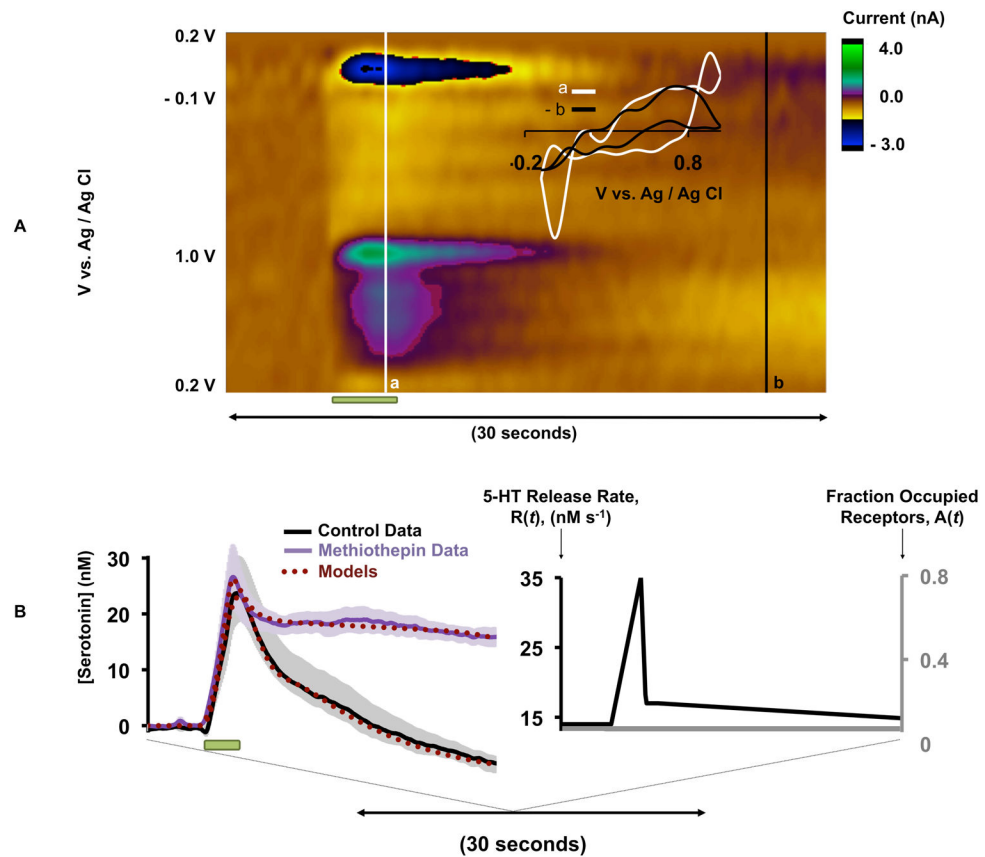


Figure 3.

A – Representative color plot of a stimulated serotonin event, stimulation duration is denoted by the green bar under the color plot. **Inset in A** – CV_a taken from the vertical white line denoted by a and superimposed onto CV_b which is taken and reversed from the vertical black line denoted by b. **B (left)** - Averaged [serotonin] vs. time (solid curves, $n=5 \pm \text{SEM}$) and modeled curves (burgundy dotted) for methiothepin treatment. Stimulation duration is denoted by the green bar under the curves. **B (right)** - $A(t) = 0$ and the choice of $R(t)$ for the methiothepin simulation.

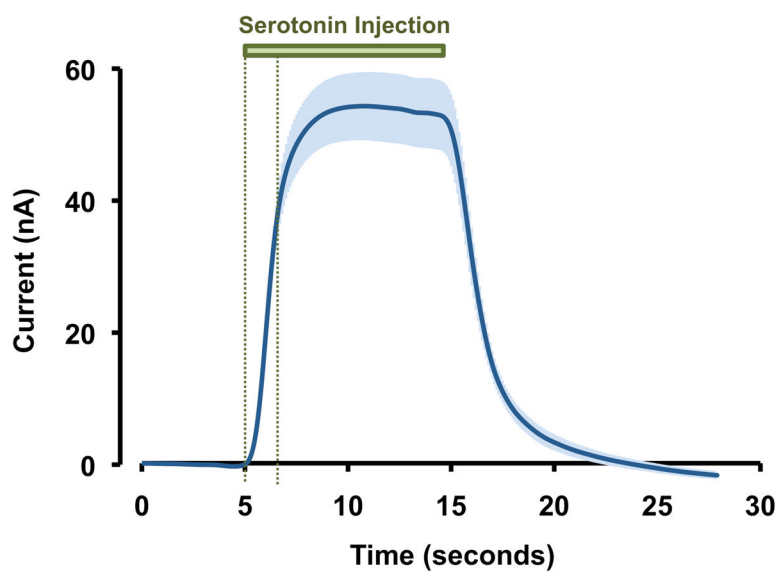


Figure 4.
In vitro FSCV response to serotonin (1 μ M) in a flow injection analysis cell (n=8 electrodes \pm SEM). The green bar indicates the duration of serotonin injection. The two vertical green dashed lines indicate the rising response portion of the signal.